Lattice Dynamics of Calcite*

E. R. Cowley† and A. K. Pant‡
Department of Physics, McMaster University, Hamilton, Ontario, Canada
(Received 9 March 1973)

The phonon dispersion relations for the lowest-ten external branches, and for wave vectors along the optic axis, have been measured in calcite, $CaCO_3$, at room temperature, by means of inelastic-neutron-scattering techniques. The results are shown to be consistent with a simple shell model containing ten adjustable parameters.

I. INTRODUCTION

The measurement of phonon dispersion relations by inelastic-neutron-scattering techniques,[1] and the calculation of the dispersion relations in terms of phenomenological force-constant models, have in recent years become routine operations for simple crystals with high symmetry and with few atoms in the unit cell. The application of the same techniques to more complicated systems is a logical step, but only a small number of such experiments have been attempted.[2]

Calcite is an obvious candidate for an investigation of this type. Its optical properties have been studied in great detail over many years. It has the properties of a typical ionic crystal, such as transparency and good cleavages, so that it is not unreasonable to attempt to calculate the phonon dispersion relations in terms of standard models of ionic crystals, such as the shell model.[3] Finally, it contains relatively tightly bound carbonate groups, so that the various branches of the dispersion curves might be expected to show the characteristics of internal and external vibrations and translational and rotational vibrations, as have been found in other cases.[4-6] The techniques, both experimental and theoretical, for dealing with these various situations have not yet completely crystallized and a further example is worth studying.

In this paper we describe the results of measurements of most of the external branches of the phonon dispersion relations in calcite, for wave vectors along the optic axis, and their interpretation in terms of phenomenological models. The structure and symmetry properties of calcite have been described elsewhere,[7] but briefly the structure is rhombohedral with 10 atoms in the unit cell and with the space group $R\bar{3}c$ (D_{3d}^6).[8] Of the 30 branches to the dispersion curves, 12 correspond to internal motions of the carbonate groups and have frequencies in the range 21.0–43.0 THz, while the remaining 18 external branches have frequencies up to a maximum of about 12.0 THz. The only direction in the lattice which has any considerable amount of symmetry is the optic axis, the [111] direction, Λ in the notation of Koster.[9]

The experimental results of measurements of the dispersion curves for this symmetry direction are described in Sec. II. A preliminary report of this work has appeared elsewhere.[10] A comparison with calculations within the shell-model formalism is made in Sec. III and the conclusions are summarized in Sec. IV.

II. EXPERIMENTS

The measurements of the phonon dispersion curves were carried out on the McMaster University triple-axis spectrometer on the NRU reactor at Chalk River.[11] The specimen was a natural rhombohedron, with a volume of approximately 40 cc, from Chihuahua, Mexico. All measurements were carried out in the constant-$\vec{Q}$ mode of operation, with the crystal at room temperature. Incident neutron energies ranging from 25 to 60 meV were used, most measurements being made at energies of 40 and 55 meV.

The experiments were confined to wave vectors along the optic axis, the [111] direction. The two reasons for this are that there are only 12 distinct external branches to the dispersion curves in this direction, since half the branches are doubly degenerate, and that the eigenvectors of the normal modes are sufficiently restricted by symmetry considerations to provide some useful selection rules in the neutron-scattering cross section. In particular, it is impossible to observe both of the quasilongitudinal Λ_1 and Λ_2 modes in the same Brillouin zone, and the doubly degenerate quasitransverse Λ_3 modes have zero cross section for $\vec{Q}$ parallel to [111]. In any other direction there are 18 branches of the dispersion curves occupying the same frequency range, and there are essentially no restrictions on the scattering structure factors, so that the problem of disentangling the various branches becomes more severe.

For all measurements the crystal was mounted with a mirror plane in the scattering plane, in order to minimize the effects of the poor out-of-plane resolution of the spectrometer. Even with this restriction we experienced considerable difficulty in measuring the doubly degenerate Λ_3 branches, the

TABLE I. Experimentally measured frequencies at Γ. All frequencies are in THz.

Optical measurements	Neutron measurements	Interpretation
2.75		$\Gamma_1'(T)$
	2.85 ± 0.10	$\Gamma_1'(T)$ and $\Gamma_3'(T)$ unresolved
3.06		$\Gamma_3'(T)$
3.69	3.53 ± 0.07	$\Gamma_3'(L)$
4.08	4.1 ± 0.1	$\Gamma_1'(L)$
4.68	4.65 ± 0.05	Γ_3
	5.17 ± 0.07	Γ_2 or Γ_2'
6.69	6.55 ± 0.10	$\Gamma_3'(T)$
7.17	7.20 ± 0.10	$\Gamma_3'(L)$
8.51	8.4 ± 0.15	Γ_3
8.90	9.05 ± 0.10	$\Gamma_3'(T)$
9.08		$\Gamma_1'(T)$
	9.26 ± 0.10	Γ_2 or Γ_2'
11.42		$\Gamma_3'(L)$
11.60		$\Gamma_1'(L)$

splitting of the degeneracy for wave vectors almost parallel to [111] causing a splitting, or at least a broadening, of the neutron groups. The most extreme case of this has been described and analyzed elsewhere,[12] but for almost all the Λ_3 branches some signs of the same effect could be detected.

To a large extent the planning of the experiments was based on a preliminary calculation of neutron-scattering cross sections, using eigenvectors calculated from a simple rigid-ion model. While these were not completely reliable, in many cases they did give the optimum positions in reciprocal space for measuring particular phonons. The interpretation of the results would have been considerably harder if these calculations had not been available. Also, during the course of the experiments recent infrared reflectivity measurements[13] were made available to us, and these greatly increased our confidence in the interpretation of the measurements.

In Table I are shown the results of the infrared[13,14] and Raman[15] scattering experiments compared with our neutron-scattering results for the point Γ ($\vec{q} = 0$). The Γ_3 modes are Raman active, while the Γ_1' and Γ_3' modes transform as the components of the macroscopic electric field. They are therefore split into transverse (T) and longitudinal (L) components, the frequencies of both being obtainable from an analysis of infrared reflectivity measurements. The Γ_2 and Γ_2' modes are neither Raman nor infrared active. We have observed two of the three external modes of these symmetries, though we are not able to distinguish between Γ_2 and Γ_2' symmetries.

The experimental results for the lowest 10 external branches are shown in Fig. 1, and some representative frequencies are given in Table II. A number of comments must be made. We believe that the fourth branch up, with a frequency of about 4.1 THz over most of the zone, is a Λ_1 branch. The neutron groups obtained for this branch were very weak and could be observed only under rather poor resolution. This is however consistent with the

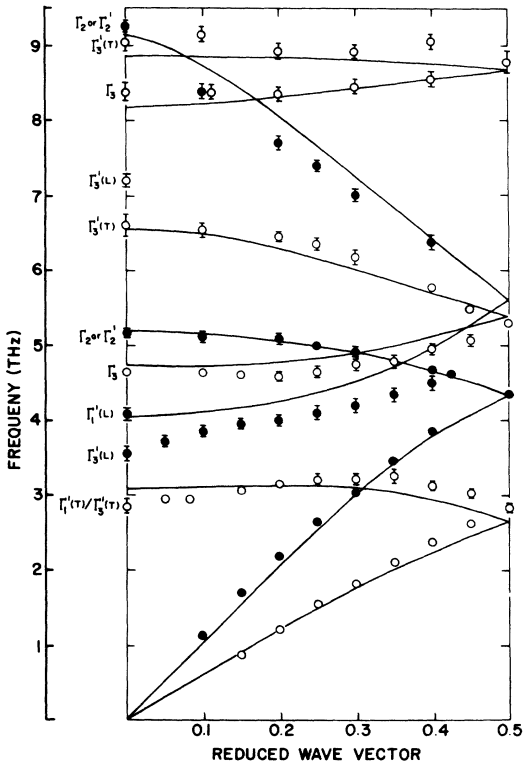

FIG. 1. Experimental and calculated dispersion curves for the Λ direction in calcite at room temperature. Full circles are Λ_1 and Λ_2 modes, open circles are Λ_3 modes. The lines are the best-fitting shell model. Probable symmetry assignments at Γ are indicated.

TABLE II. Experimental frequencies at reduced wave vectors of 0.25, 0.25, 0.25 and 0.5, 0.5, 0.5.

$\vec{q}=0.25, 0.25, 0.25$		$\vec{q}=0.5, 0.5, 0.5$	
Frequency	Symmetry	Frequency	Symmetry
1.53 ± 0.05	Λ_3	2.86 ± 0.06	Z_2/Z_3
2.61 ± 0.05	Λ_1	4.30 ± 0.06	Z_1
3.25 ± 0.10	Λ_3	5.25 ± 0.07	Z_2/Z_3
4.09 ± 0.10	Λ_1	5.5 ± 0.2	Z_1[a]
4.56 ± 0.07	Λ_3	8.75 ± 0.15	Z_2/Z_3
5.00 ± 0.08	Λ_2		
6.35 ± 0.10	Λ_3		
7.4 ± 0.15	Λ_2		
8.4 ± 0.1	Λ_3[a]		
8.95 ± 0.1	Λ_3[a]		

[a]Interpolated.

calculated structure factors. In the model calculation this branch is predominantly a rotational branch and gives rise to structure factors, over the whole available region of $\vec{Q}$ space, which are smaller than those for any other modes which we were able to observe. The intensity of the observed groups dropped as the zone boundary was approached, but if our identification is correct this branch must become degenerate at the zone boundary with a Λ_2 branch (eighth branch up over most of the zone), at a zone-boundary frequency of about 5.5 THz. We were however unable to observe this zone-boundary frequency, partly because it is close in value to a Z_2/Z_3 mode, and we could not with confidence distinguish two separate frequencies.

Secondly, we believe that the shape near $\vec{q}=0$ of the two lowest optical branches is governed by resolution conditions. These branches are both infrared active and thus modes with wave vectors very close to $\vec{q}=0$ have frequencies which depend strongly on the direction of the wave vector. In a neutron-scattering experiment the measurement actually at $\vec{q}=0$ samples both transverse and longitudinal modes, and if the frequencies are not well separated, gives an average value for the frequency. The dip in the lowest Λ_1 optical branch near $\vec{q}=0$ then represents the difference between this average value of about 3.6 THz at $\vec{q}=0$, and the true longitudinal value of about 4.1 THz for $\vec{q}$ of 0.15 or greater. The results given in Table I are based on measurements made at or near a large number of reciprocal lattice points, in order to unscramble the results as far as possible.

The experimental values at frequencies of 4.1 and 7.2 THz, at $\vec{q}=0$, were extracted in this way, and do not connect smoothly with other measurements made at small but finite wave vectors. The mode at 7.2 THz represents the end point of a branch of the dispersion curve in directions perpendicular to [111], and the point at 4.1 THz represents the true end point of the Λ_1 branch which was actually observed, in the typical run shown, as dipping down towards the $\Gamma_3'(L)$ frequency of 3.53 THz.

The final area where some uncertainty exists concerns the Γ_2 or Γ_2' frequency (a black dot) at 9.26 THz. We are unable to distinguish between Γ_2 and Γ_2' modes, both being compatible with the Λ_2 branch. However, the calculations suggest that there are two such frequencies close together and that we have observed the upper one. In that case the solid line is incorrectly fitted, and the mode at 9.26 THz is the starting point of the 11th branch of the dispersion curve. The Λ_2 branch would then approach $\vec{q}=0$ at a lower frequency. We have searched for such a lower frequency and at the moment it appears to us that the only possibility is that the mode at 7.2 THz contains a contribution from this source. However the most likely connectivity is that shown in the figure.

III. THEORY

We have attempted to analyze the experimental results in terms of a shell model.[3] The systematic application of such a model to a complicated structure would involve a very large number of adjustable parameters, whereas the number of parameters which can be determined from the data available is limited, probably to about 12. It is therefore necessary to make drastic assumptions to keep the number of unknowns to about this level. Undoubtedly the values obtained for the surviving parameters depend sensitively on these assumptions. The present calculations are therefore to be regarded as illustrating the type of results of which the shell model is capable, rather than being a definitive model of calcite.

The form of shell model used was similar to that applied by one of us to ammonium chloride.[16] In particular short-range forces between the shells were omitted and the equation of motion was written in the form

$$\underline{m}\omega^2\underline{U} = [(\underline{R}+\underline{Z}\underline{C}\underline{Z}) - (\underline{T}\underline{Y}^{-1}+\underline{Z}\underline{C})\alpha(\underline{1}+\underline{\mathfrak{C}}\,\alpha)^{-1} \times (\underline{Y}^{-1}\underline{T}^{+}+\underline{C}\underline{Z})]\underline{U} \ .$$

Here $\underline{m}$ and α are diagonal matrices of ionic masses and polarizabilities. The values used for the polarizabilities were derived from an analysis of refractive-index data.[17] $\underline{\mathfrak{C}}$ is a matrix of Coulomb coefficients calculated using the Ewald transformation and $\underline{C}$ is a similar matrix satisfying translational invariance conditions. $\underline{Z}$ is a diagonal matrix of ionic charges and $\underline{Y}$ is a diagonal matrix of shell charges. Actually all of our calculations were programmed in terms of the reciprocals of the shell charges, and $\underline{Y}^{-1}$ for the carbon ion was taken to be zero. This is equivalent to neglecting the short-range polarizability of the

carbon. The $\underline{T}$ matrix was assumed to be equal to the $\underline{R}$ matrix, which contains the short-range contributions to the dynamical matrix, although it must be remembered that, since $\underline{T}$ occurs only in the combination $\underline{T}\underline{Y}^{-1}$, and $\underline{Y}^{-1}$ is zero for the carbon atom, the values assumed for the rows of $\underline{T}$ referring to carbon motion are immaterial.

In the $\underline{R}$ matrix we include force constants describing the non-Coulomb intramolecular forces of a carbonate group, and two-body, or axially symmetric, forces describing the interactions of a calcium ion with the six nearest-neighbor oxygen ions, and the interactions of an oxygen ion with the shell of six nearest oxygen ions in the same plane, and with the next shell of six oxygen neighbors out of the plane. The values of the intramolecular force constants were obtained from the frequencies of the internal vibrational frequencies, and were not fitted to the external modes. The intermolecular forces required a total of six parameters.

All of the matrices referred to above have dimensions of 30×30, since an independent-atom formalism was used, rather than one in which the carbonate groups were treated as rigid. We feel that the combination of a shell model with a rigid molecule model has not yet been justified. In the case of the carbonate ion the highly polarizable oxygen ions sit on the outside of the group, and it does not seem reasonable to describe their polarizations in terms of the motion of a single shell centered on the carbon ion. The refractive-index analysis[17] also indicates that a single central shell is not a meaningful picture.

The model contains 10 parameters to be fitted to the experimental dispersion curves: six short-range interatomic force constants, two independent ionic charges (chosen to be the calcium charge and the carbon charge), and two shell charges. There are, in addition, three ionic polarizabilities and six intramolecular force constants whose values are obtained externally. The parameters were adjusted in a nonlinear least-squares fit to the experimental data. Two fits were carried out with the long-wavelength frequency of 9.26 THz taken to be either a Γ_2 or a Γ_2' mode. The quality of fit obtained was almost identical in the two cases, though marginally better when the mode was assumed to be of Γ_2' symmetry, and the parameter values obtained in the two fits were all the same within their standard deviations. The results for the best-fitting model are shown in Fig. 1. The quality-of-fit parameter χ had the value 2.71 for this model.

As stated above, the exact values of the parameters undoubtedly depend greatly on the details of the models used. A complete description is therefore relegated to the Appendix. Some general observations are in order. The values obtained for the ionic charges in the best model are $+2.3e$ for the calcium ion, close to its formal value, and $+0.27e$ for the carbon ion. The charge on the oxygen ions is then $-0.87e$. These charges correlate well with the values assumed for the ionic polarizabilities.[17] We emphasize that the ionic polarizability values do give the correct values for the refractive indices. Plihal and Schaack[14] found it necessary to use much smaller values for the polarizabilities in their calculations of the frequencies at Γ.

IV. DISCUSSION

The experimental results described in Sec. II do not have the unambiguous nature to which one has grown accustomed in neutron-scattering experiments. The three reasons for this are worth repeating. First, the low symmetry of the crystal results in a nonvanishing out-of-plane component of the gradient of the dispersion curves, leading to a broadening or even a splitting of the Γ_3 modes. Where adequate intensity is available the instrumental resolution can be improved, but this is not always possible. Second, the large number of atoms in the unit cell, at sites of low symmetry, leads to the structure factor being nonperiodic in reciprocal space, and the presence of rotational modes results in the structure factors for some modes being small at all accessible points in reciprocal space. The result of this is that some modes could be measured in only one area of reciprocal space, whereas measurements made at several points would be preferred when the interpretation of a neutron group is in doubt. The procedure for finding the best points in reciprocal space consisted in part of using a preliminary calculation of structure factors and in part of making extended scans at a large number of points in reciprocal space for one or two reduced wave vectors.

The third major difficulty arose from the splittings of the infrared-active optical modes at long wavelengths, into transverse and longitudinal components. Because of the rather poor resolution of a triple-axis spectrometer it is unavoidable that in measurements at small wave vectors the observed neutron groups contain contributions from modes of unwanted polarizations and frequencies. Consider for example the highest-frequency Λ_3 branch. The branch is doubly degenerate and as $\vec{q}$ tends to zero along the Λ direction the end point of the branch is the doubly degenerate $\Gamma_3'(T)$ mode. Out of the top of the figure is a Λ_1 branch terminating at $\vec{q}=0$ in the $\Gamma_1'(L)$ frequency of 11.60 THz. However for $\vec{q}$ tending to zero along a direction perpendicular to Λ, the Γ_3' mode is split into transverse and longitudinal components, the longitudinal frequency being 11.42 THz, while the Γ_1' mode has the transverse frequency of 9.08 THz. Thus for small wave

TABLE III. Parameter values in the best-fitting shell model.

Parameter	Units	Value
A_1	10^4 dyn/cm	11.824
B_1	10^4 dyn/cm	−1.022
A_2	10^4 dyn/cm	−0.422
B_2	10^4 dyn/cm	−0.273
A_3	10^4 dyn/cm	0.309
B_3	10^4 dyn/cm	0.142
A_{CO}	10^4 dyn/cm	36.0
B_{CO}	10^4 dyn/cm	65.5
C_{CO}	10^4 dyn/cm	18.0
A_{OO}	10^4 dyn/cm	13.6
Z_{Ca}	$\|e\|$	2.348
Z_C	$\|e\|$	0.266
Y_{Ca}	$\|e\|$	2.132
Y_O	$\|e\|$	−2.291
α_{Ca}	Å^3	0.968
α_C	Å^3	0.073
α_O	Å^3	1.204

vectors, as the direction of $\vec{q}$ changes from Λ to a direction perpendicular to Λ, the frequency of the upper branch will change from 11.60 to 11.42 THz, while the Λ_3 branch will split into two branches, the frequency of one remaining at the $\Gamma_3'(T)$ value while the frequency of the other changes smoothly to the $\Gamma_1'(T)$ value. A comparison of the numbers given in Table I indicates that our value of 9.05 THz is probably an average of the $\Gamma_3'(T)$ and $\Gamma_1'(T)$ frequencies. It would be interesting to see the results of a convolution of an instrumental resolution function with a set of split dispersion curves of this nature. Clearly, however, the techniques of Raman scattering and infrared reflectivity measurement provide less ambiguous measurements of the long-wavelength modes in such a crystal.

By contrast the shell-model calculations were relatively straightforward. However the difficulty in this part of the work was in finding a set of parameters which lead to stable dispersion curves. Once these had been found the least-squares procedure converged quite well, but it would have been impossible to use the shell model in the preliminary calculations of structure factors. The dispersion curves of the rigid-ion model used in the preliminary calculations were not a good fit to the experimental curves, but on the other hand no difficulty was encountered in setting up a stable model.

ACKNOWLEDGMENTS

This work was performed while the authors were research associate (E. R. C.) and postdoctoral fellow (A. K. P.) at McMaster University. The authors are grateful to Dr. B. N. Brockhouse for providing financial support, experimental facilities, and helpful advice.

APPENDIX

We give here more details of the shell model used in the calculations described in Sec. III.

The contributions to the R matrix consist of intramolecular force constants of the carbonate group and near-neighbor interatomic force constants between atoms not in the same group. The latter are treated as axially symmetric, so that the force constant $\phi_{xy}(i,j)$ between atoms i and j, a distance r apart and separated by a vector (x, y, z) is

$$\phi_{xy}(i,j) = -(xy/r^2)(A_n - B_n) - \delta_{xy}B_n \ .$$

Three sets of A_n and B_n are used. A_1 and B_1 refer to the interaction of a calcium ion with the six nearest-neighbor oxygen ions, A_2 and B_2 refer to the interaction of an oxygen ion with the six nearest oxygen ions in the same basal plane, and A_3 and B_3 refer to the interaction of an oxygen ion with the six nearest oxygen ions not in the same plane.

There are, in addition, the intracarbonate force constants. If a CO_3 group is oriented perpendicular to the z axis, with one carbon oxygen bond in the y direction, the force-constant matrix describing that interaction is

$$-\begin{pmatrix} A_{CO} & 0 & 0 \\ 0 & B_{CO} & 0 \\ 0 & 0 & C_{CO} \end{pmatrix} .$$

In the same orientation the force-constant matrix describing the interaction between the other two oxygen atoms is

$$-\begin{pmatrix} A_{OO} & D_{OO} & 0 \\ -D_{OO} & B_{OO} & 0 \\ 0 & 0 & C_{OO} \end{pmatrix} .$$

The potential energy of the carbonate group is rotationally invariant if

$$C_{CO} + 3C_{OO} = 0 \ ,$$

$$A_{CO} + 3B_{OO} + (\sqrt{3})D_{OO} = 0 \ .$$

There are thus five independent parameters. An isolated CO_3 group has only four distinct vibrational frequencies. If the forces were axially symmetric D_{OO} would be zero. We therefore arbitrarily set this parameter to zero and then determined the other six parameters. The values so obtained are included in Table III. These are the total force constants and before the appropriate contributions are included in the R matrix a rigid-ion Coulomb contribution to these constants is subtracted. This is still not exact since there are also shell-model correction terms. As a result our model does not give all of the internal frequencies

exactly. This was however not considered to be of importance in a calculation of the external frequencies. A complete listing of the parameter values in the best model is given in Table III.

---

*Work supported by the National Research Council of Canada.
†Present address: Dept. of Physics, Brock University, St. Catharines, Ontario, Canada.
‡Present address: Dept. of Physics, University of Gorakhpur, Gorakhpur, U. P., India.

[1]B. N. Brockhouse, in *Phonons in Perfect Lattices and in Lattices with Point Imperfections*, edited by R. W. H. Stevenson (Oliver and Boyd, London, 1966).
[2]For example, M. M. Elcombe, Proc. Phys. Soc. Lond. **91,** 947 (1967); J. D. Axe and G. Shirane, Phys. Rev. B **1,** 342 (1970).
[3]A. D. B. Woods, W. Cochran, and B. N. Brockhouse, Phys. Rev. **119,** 980 (1960).
[4]G. Venkataraman and V. C. Sahni, Rev. Mod. Phys. **42,** 409 (1970).
[5]G. Dolling and B. M. Powell, Proc. R. Soc. A **319,** 209 (1970).
[6]H. C. Teh and B. Brockhouse, Phys. Rev. B **3,** 2733 (1971).
[7]E. R. Cowley, Can. J. Phys. **47,** 1381 (1969).
[8]R. W. G. Wyckoff, *Crystal Structures* (Interscience, New York, 1948).
[9]G. F. Koster, Solid State Phys. **5,** 173 (1957).
[10]A. K. Pant and E. R. Cowley, Acta Crystallogr. A **25,** S28 (1969).
[11]B. N. Brockhouse, G. A. DeWit, E. D. Hallman, and J. M. Rowe, in *Neutron Inelastic Scattering* (International Atomic Energy Agency, Vienna, 1968), Vol. II.
[12]E. R. Cowley, and A. K. Pant, Acta Crystallogr. A **26,** 439 (1970).
[13]K. H. Hellwege, W. Lesch, M. Plihal, and G. Schaack, Z. Phys. **232,** 61 (1970).
[14]M. Plihal and G. Schaack, Phys. Status Solidi **42,** 485 (1970).
[15]L. Giulotto, and G. Olivelli, Nuovo Cimento **5,** 52 (1948).
[16]E. R. Cowley, Phys. Rev. B **3,** 2743 (1971).
[17]E. R. Cowley, Can. J. Phys. **48,** 297 (1970).